Accepted Manuscript

New insights into electrocatalytic ozone generation via splitting of water over PbO_2 electrode: A DFT study

Gregory Gibson, Ashley Morgan, P. Hu, Wen-Feng Lin

Please cite this article as: G. Gibson, A. Morgan, P. Hu, W-F. Lin, New insights into electrocatalytic ozone generation via splitting of water over PbO_2 electrode: A DFT study, *Chemical Physics Letters* (2016), doi: http://dx.doi.org/10.1016/j.cplett.2016.04.078

New insights into electrocatalytic ozone generation via splitting of water over PbO_2 electrode: A DFT study

Gregory Gibson[a,b], Ashley Morgan[b], P. Hu[b] and Wen-Feng Lin[a,b*]

[a] *Department of Chemical Engineering, Loughborough University, Loughborough, Leicestershire, LE11 3TU, UK.*

[b] *Centre for the Theory and Application of Catalysis, School of Chemistry and Chemical Engineering, Queen's University of Belfast, Belfast BT9 5AG, U.K.*

Abstract

The viable mechanisms for O_3 generation via the electrocatalytic splitting of H_2O over β-PbO_2 catalyst were identified through Density Functional Theory calculations. H_2O adsorbed onto the surface was oxidized to form OH then O; the latter reacted with a surface bridging O to form O_2 which in turn reacted with another surface O to form O_3. The final step of the mechanisms occurs via an Eley-Rideal style interaction where surface O_2 desorbs and then attacks the surface bridging oxygen, forming O_3. A different reaction pathway via an O_3H intermediate was found less favoured both thermodynamically and kinetically.

Keywords: Electrochemical Ozone Production, Density Functional Theory, Advanced Oxidation Technology, Lead Oxide, Activation Energy, Reaction Pathway

*Corresponding author at Loughborough University: E-mail: w.lin@lboro.ac.uk (W. F. Lin).

1. Introduction

Ozone (O_3) is a strong oxidant with wide applications across many disciplines related to advanced oxidation technologies. Due to its strong oxidizing nature O_3 is often used in disinfection processes at wastewater treatment facilities. It has relevance in removing unwanted odours, wood pulp bleaching and more recently in healthcare [1-6]. For practical uses, O_3 must be produced in an efficient and environmentally friendly manner, which to date has proven to be the greatest challenge. At present O_3 is produced industrially via the Cold Corona Discharge (CCD) method. This process involves two electrodes with alternating current, similar to an electric spark, with pure oxygen (O_2) or dry air passing between them. Current efficiency (CE) values tend to be low at between 2-12 wt% depending on the source of O_2 [7, 8].

Through the use of electrochemistry and in particular, electrocatalysis, a superior O_3 yield can be achieved via water splitting. In electrolysis, H_2O undergoes decomposition at the anode through either a 4 or 6 electron process shown in reactions 1 and 2 [9]:

$$2H_2O \longrightarrow O_2 + 4H^+ + 4e^- \qquad E^o = 1.23 \text{ V} \qquad (1)$$

$$3H_2O \longrightarrow O_3 + 6H^+ + 6e^- \qquad E^o = 1.51 \text{ V} \qquad (2)$$

Reaction (1) shows the competing reaction, the formation of O_2 that can occur instead of the formation of O_3 in reaction (2). This can be quantified using thermodynamics. In comparison to O_3, O_2 is thermodynamically superior in terms of stability and thus will readily form. To combat this, the inhibition of O_2, and hence the formation of O_3 is of paramount importance. By running at a high onset potential with a large applied overpotential the thermodynamic barrier can be bypassed, resulting in O_3 formation. In selecting a suitable catalyst for the anode, the overpotential required for oxygen evolution reaction (OER) can be increased. During the production of O_3, the increased overpotential required for OER results in partial inhibition of the oxygen evolution when compared to a material with a lower overpotential for OER [10, 11]. Extensive research on catalyst suitability has been studied with varying degrees of success. Among the most common catalysts used are β-PbO_2 [10-12], Pt [13], dimensionally stable anodes (DSAs) [14], boron-doped diamond [15, 16] and SnO_2 based

2

catalysts [17-19]. Foller et al., one of the pioneering groups in the study of electrochemical O_3 formation, used β-PbO_2 as the catalyst of choice. Using new and innovative methods O_3 was produced electrochemically. Foller summarised his research into four points:

- The anion must be resistant to further oxidation, or oxidize into a species that doesn't decrease the yield
- The cation must undergo no cathodic reduction, nor be influenced by pH change
- Salt combinations must have sufficient solubility
- No reactions with the ozone produced must occur

Previous methods produced O_3 in low yield, resulting in low CEs. β-PbO_2 was the first to achieve a better CE than the CCD method, with values as high as 13 % at room temperature [10]. Higher efficiencies were possible with the addition of a fluorinated anion; yielding CEs as high as 50 %, although this occurred at 0 $^\circ$C. As the goal is to produce highly efficient anodes whilst being as green as possible, the use of fluorine or other halogens are disapproved.

Although in these studies a significant amount of understanding has been gained there are still questions that need to be answered:

- Is the mechanism postulated correct or will it proceed via an alternative pathway?
- Are there any surface oxidants present?
- What role do these oxidants/adsorbents play?

The focus of this research is to address these questions within the parameters that can be studied using theoretical methods, with the aim to gain a reasonable yet computationally affordable approach to understanding the electrochemical O_3 production system, which has proven difficult to achieve in the past, and thus difficult to model. With this work being novel as a first theoretical study, simulations had to be run in order to determine the most stable facet of the PbO_2 anode, along with the optimal surface oxygen coverage. From this a phase diagram can be constructed which aids in determining surface oxidant coverage, which in turn is important for modelling the reaction.

The main purpose of this research involved the modelling of a 4 step mechanism where water can be split to form O_3 under the suitable electrochemical conditions. The modelling was carried out using Density Functional Theory (DFT). β-PbO_2, the experimentally approved

3

catalyst of choice for this reaction, was chosen. It is a relatively simple system where the results gained could then be applied to more complex catalysts.

2. Theoretical Methods

2.1. Surface Adsorption Calculations

The adsorption energy (E_{ads}) was calculated using the following equation:

$$E_{ads} \text{ (adsorbate)} = E \text{ (adsorbate on surf.)} - E \text{ (surf.)} - E \text{ (free adsorbate in the gas phase)} \tag{3}$$

Equation 3 shows that the more negative the adsorption energy is, the greater the adsorption to the surface. In this instance it can be a clean surface or an oxide surface, depending upon the study. Each term in the equation must correspond to the same surface coverage, whether this is a pure metal or metal oxide.

Geometric optimization was obtained by performing electronic structure calculations using the *Vienna Ab-initio Simulation Package (VASP)*, using plane wave basis set [20-22]. Electron exchange and correlation terms were described using the *Perdew-Burke-Ernzerhof* (PBE) functional [23]. Electron-ion interactions were modelled using the *projected augmented wave* (PAW) potential with system converging with cut-off energy of 500 eV [24].

The ground state was determined using Methfessel-Paxton smearing of 0.05 eV [25]. The most stable β-PbO_2 system was a (110) surface. This was modelled as a (2x2) unit cell on surface coverage's barring the 0.125 ML (ML = mono-layer) coverage. This coverage employed the use of a super cell modelled as a (4x2) unit cell. The k-points for the surfaces with (2x2) unit cell were sampled using a 3x3x1 Monkhorst-Pack grid [26] with the super cell having k-points 1x3x1. A four-layered slab was employed, with the bottom two layers fixed in geometry, whereas top two layers were allowed to relax. Slab separation was provided normal to the surface by use of a 15 Å vacuum region. Transition state (TS) searching was implemented using a constrained minimisation method [27-29].

3.Results and Discussion

3.1. Determination of the most stable facet of PbO₂

PbO$_2$ can exist in two crystalline forms; the alpha version which is orthorhombic and the beta version which is tetragonal in shape. It has been suggested that the beta version is the more favoured structure for O$_3$ evolution. The alpha form is said to have better contact between particles, due to its more compact structure in comparison with the beta form. This compactness results in difficulty with discharge. For these reasons the beta form is often used when carrying out O$_3$ evolution [30] .

Although studies on other surfaces were carried out, Foller and Tobias focused on exploring β-PbO$_2$ as their catalyst of choice for O$_3$ evolution. Other groups have also studied this system experimentally; however there are no examples in the literature studied on a theoretical level. Before modelling the reaction, the most stable surface facet had to be calculated. As this work is the first theoretical attempt, data on surface stability or morphology was lacking, so some common surface geometries were tested. The surface of β-PbO$_2$ is analogous to SnO$_2$, which has been studied previously. The (110) facet is reported as the most stable for SnO$_2$, so this was chosen as a sensible starting point. The four arrangements tested were (110), (111), (100) and (211) mono-atomic step edge facets.
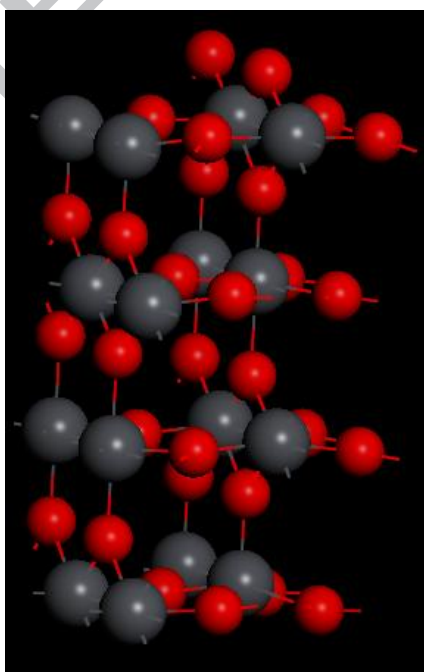

Figure 1. *A diagram showing β-PbO$_2$ (110), the most stable surface facet, modelled as a four layer system. The grey atoms represent lead, and the red atoms represent oxygen.*

Upon calculation of these different facets, the most stable one was found to be the (110) facet (Figure 1) and therefore this is the surface that the mechanism was modelled upon.

3.2. Surface oxidants

After calculating a stable facet, formation of surface oxidants from water adsorption and activation can be calculated which in turn can be useful in constructing a phase diagram (Figure 2). β-PbO_2 (110) has four lead sites on its surface, two on the top site region and two on the bridging region. It is therefore possible to have 0.25, 0.50, 0.75 and 1 ML surface oxidant coverage.

The main surface oxidants expected are either O or OH or both at the same time. As this is oxidation reaction, it is loss of electrons and therefore a proton is released in step 1 of the mechanism. Although unlikely, there is the possibility of surface H^+ and this must also be taken into account.

3.2.1. Construction of a phase diagram showing surface oxidant formation

Each calculation will yield an energy value; this is the total energy of the system. When constructing a phase diagram, it is the free energy that is required. The free energy change (ΔG) of the system can be calculated using equation 4:

$$\Delta G = \Delta E + ZPE - T\Delta S \tag{4}$$

ΔE is the total energy change, ZPE is zero-point energy and the $T\Delta S$ is the temperature and the change of the entropy of the system. The free energy change of the system accounts for the zero-point energy and the entropy associated. Temperature is also factored into this, along with a pH correction factor, as experimentally the reaction is carried out in acidic electrolyte.
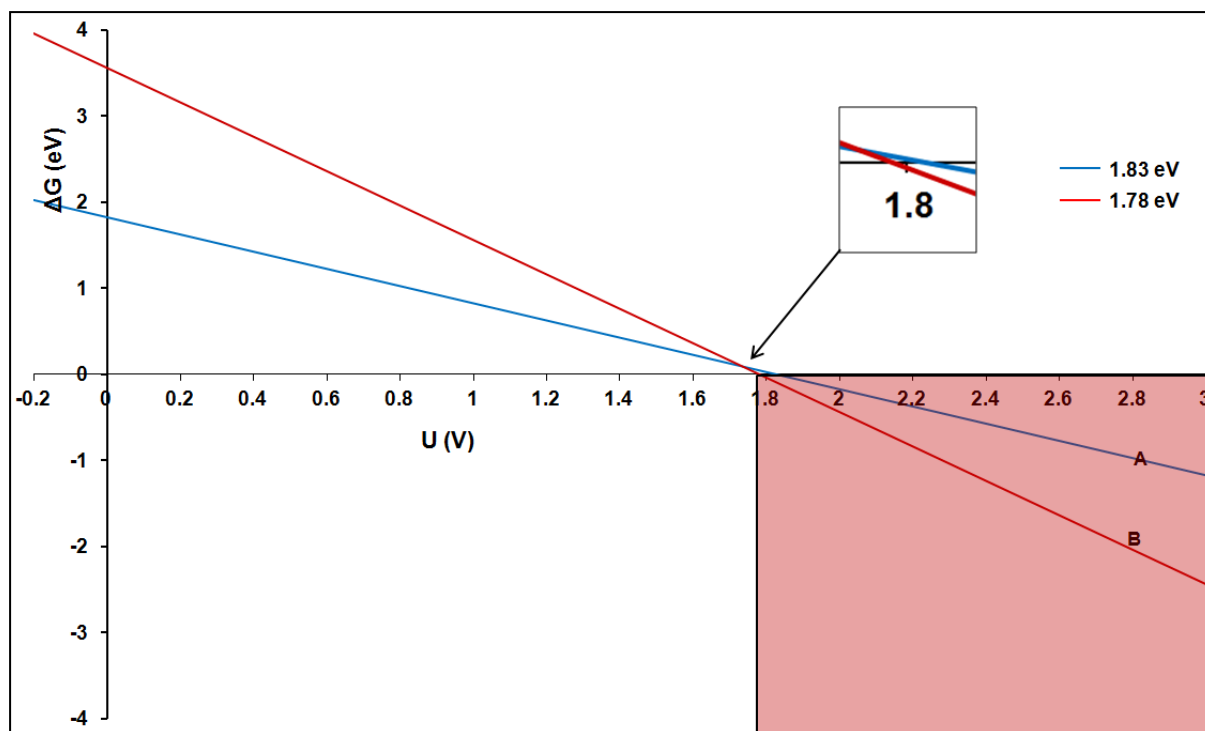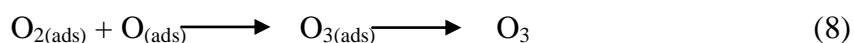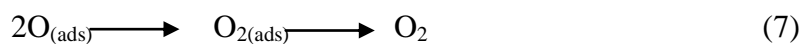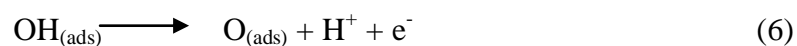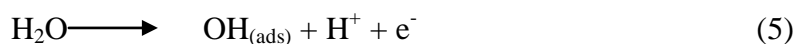
6

Figure 2. *Plot of ΔG of formation of surface oxidants against applied potential (vs. SHE) on the β-PbO₂ surface. The blue line (line A) represents the stability of adsorbed OH with potential and the red line (line B) represents the stability of adsorbed O with potential. The white area (ΔG > 0) represents the potential region where no surface oxidants are present and the red area (ΔG < 0) represents the potential region in which O is the predominant surface oxidant.*

3.3. A comparison of the formation of O_3 via two different pathways

The mechanism being modelled has four steps that involve the splitting of H_2O to O_2 (ads) intermediate before forming O_3 through the interaction with further surface O. This is better illustrated in reactions 5-8:

$$H_2O \longrightarrow OH_{(ads)} + H^+ + e^- \tag{5}$$

$$OH_{(ads)} \longrightarrow O_{(ads)} + H^+ + e^- \tag{6}$$

$$2O_{(ads)} \longrightarrow O_{2(ads)} \longrightarrow O_2 \tag{7}$$

$$O_{2(ads)} + O_{(ads)} \longrightarrow O_{3(ads)} \longrightarrow O_3 \tag{8}$$

The first two steps (reactions 5 and 6) happen almost simultaneously as a fixed potential is applied across the anode surface. The main focus of this study is steps 3 and 4 (reactions 7 and 8). Step 3 is the formation of O_2 as shown in Figures 3 and 4, and step 4 is the formation of O_3 from the O_2 formed in step 3 and further surface O, as shown in Figure 5.
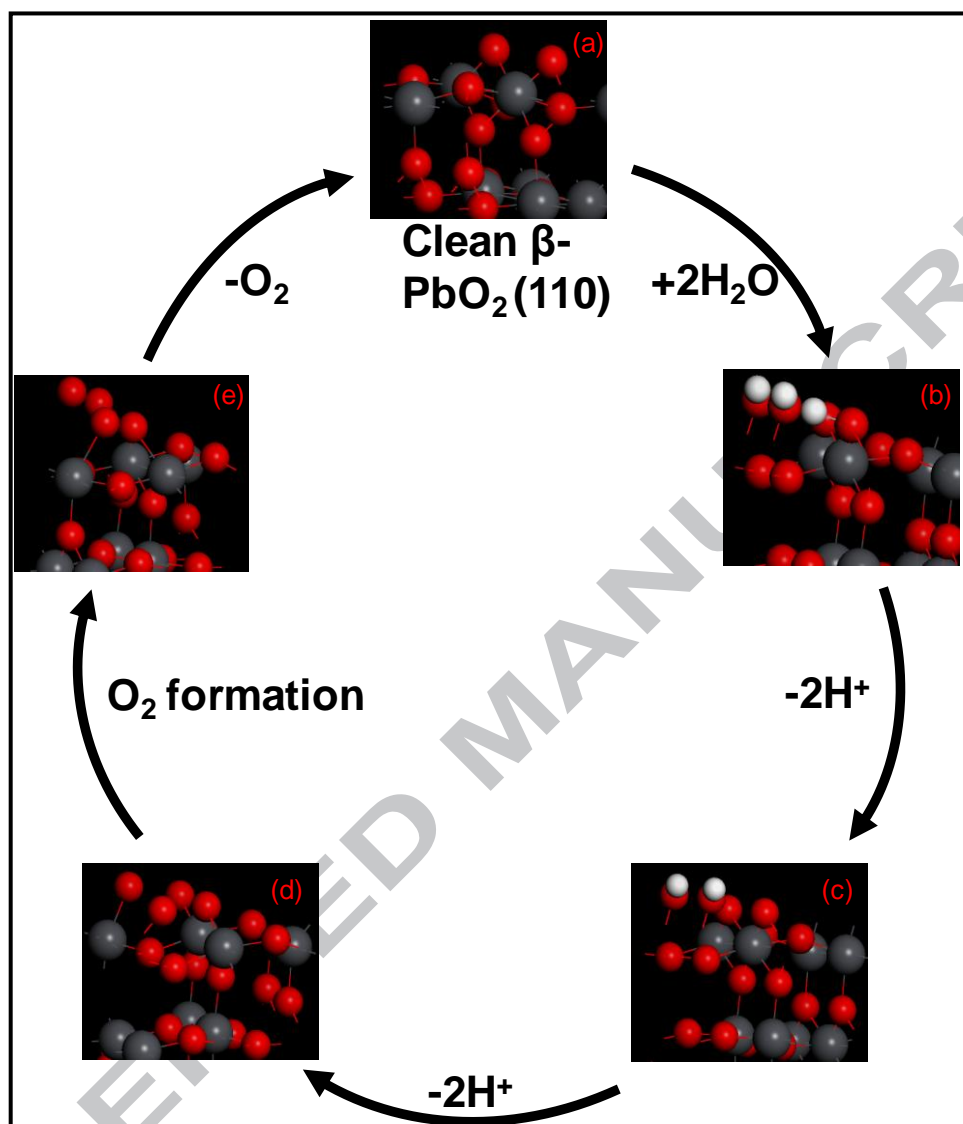
Figure 3. *A flow mechanism showing steps 1 to 3 of the overall mechanism. (a) is the clean surface, (b) shows the adsorption of H_2O, (c) shows the deprotonation of one H, (d) shows the deprotonation of the second H and (e) shows the formation and subsequent desorption of O_2 back to the clean surface*

3.3.1. Step 3 – The formation of O_2 via the combination of two surface O atoms

In this step there are two oxygen atoms on the surface that combine to form O_2.

$$2O_{(ads)} \longrightarrow O_{2(ads)} \longrightarrow O_{2(gas)} \qquad (9)$$
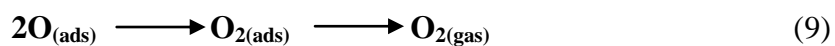
In all chemical reactions there is an initial state (IS), transition state (TS) and final state (FS). The initial state is the starting point, the transition state is when the surface adsorbates are highest in potential energy and the final state is one in which the desired reaction has reached completion. In this case the IS was the adsorbed O along with bridging O, and the FS will be surface adsorbed O_2. Upon completion of the calculations a reaction profile can be constructed:

Initial state of reaction

The initial mechanistic step involves two bridging oxygen atoms on the original surface and 0.50 ML coverage of oxygen present on the top site region. The bond distance between top-site and bridging is 2.199 Å. The energy associated with its stable configuration was calculated to be -258.95 eV.

Transition state

The TS was identified as the point that is highest in energy. In this case it can be described as the point in which the two adjacent O atoms are closest without bond formation taking place. By using computational methods a suitable TS can be identified. After calculating an adsorbates most stable geometry, i.e., a geometry optimization, a frequency calculation can be run. The outcome of these calculations should result in a number of determined frequency values, depending on the level of surface coverage. Of these frequency values, at least one should be an imaginary frequency (f/i). If all frequencies calculated are real then the configuration tested is, in fact, not a TS and so adjustments need to be made, the most common of which is to configure the bond distances.
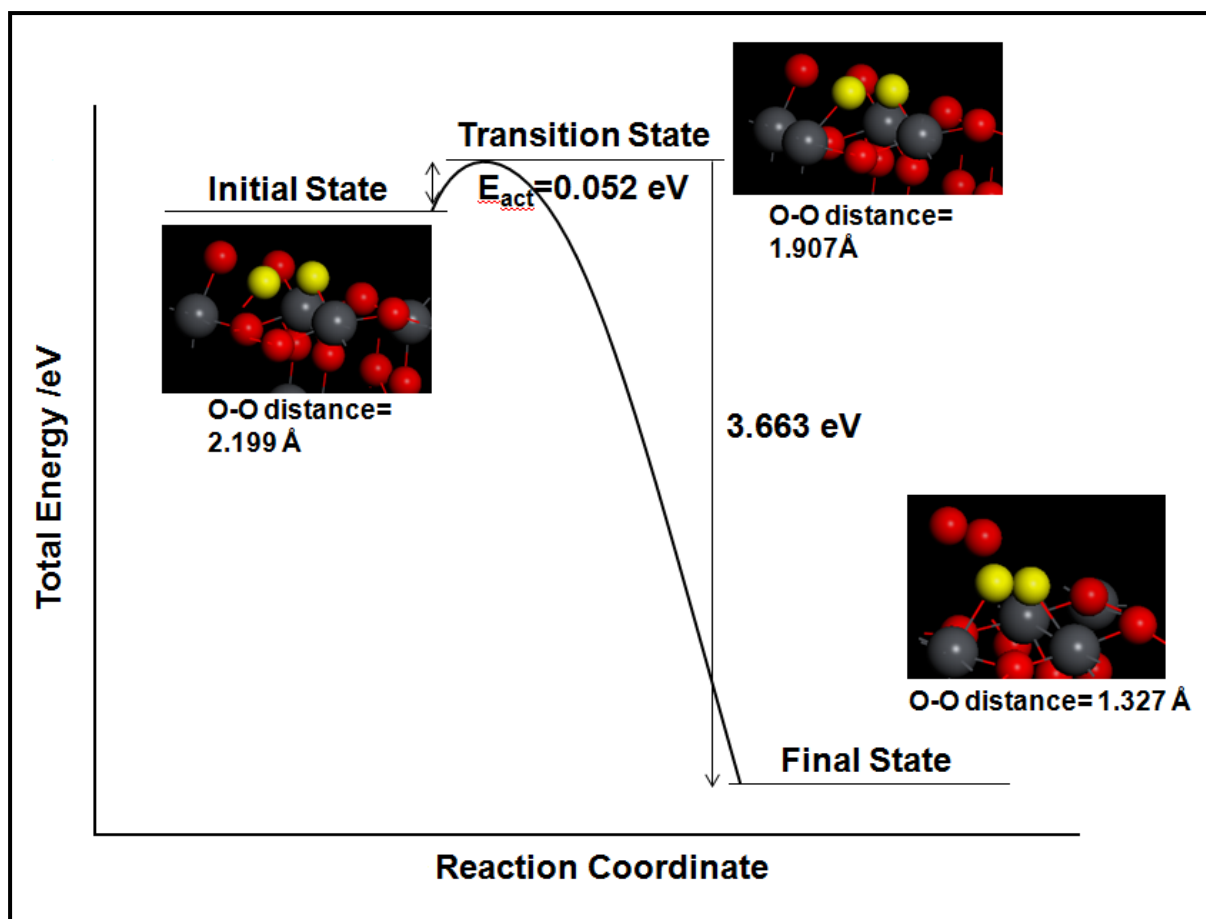
Figure 4. *Energy profile for step 3 of the mechanism: the formation of surface O_2 from two adsorbed oxygen atoms. The atoms highlighted in yellow are the interacting O atoms in the mechanism. The initial state shows the adsorbed O and bridging surface O, the transition state shows both these atoms in a closer proximity to one another, and the final state shows both atoms bonded to form surface O_2.*

The progression from IS to TS will have an activation energy (E_{act}) associated with it. This barrier can be determined by taking IS away from the TS:

$$\mathbf{E_{act}} = E_{TS} - E_{IS} = (-258.90) - (-258.95) = 0.05 \text{ eV} \tag{10}$$

For step 3 the activation barrier was calculated at only 0.05 eV. Thermodynamically the progression from IS to TS will occur with ease. Both the TS and IS have similar properties and so there is little change structurally, barring the bond lengths between the two states (Figure 4).

10

Final state of reaction

The FS of step 3 shows the formation of surface adsorbed O_2. This occurs via the reaction of the same top site-bridging oxygen interaction seen in the IS. The resulting structure shows the successful formation of O_2, with the non-interacting oxygen atoms forming O_2 on the surface. As a result little O_2 remains adsorbed whereas the majority will desorb. This is what is expected to happen as for β-PbO_2, CE values struggle to reach 10 %. This suggests that for every one hundred O_2 formed only ten will remain adsorbed.

The enthalpy change (ΔH) associated with the overall reaction from the IS to the FS was calculated in equation 11:

$$\Delta H = E_{FS} - E_{IS} = (-262.61) - (-258.95) = -3.66 \text{ eV} \tag{11}$$

A value of -3.66 eV would suggest that the FS is more stable than the IS and thus the reaction from IS to FS is exothermic.

After formation of surface O_2 the adsorption energy can be calculated to determine the strength of adsorption (equation 12).

$$\begin{aligned} E_{ads}(O_2) &= E \text{ (surface } O_2) - E \text{ (clean surface)} - E(O_2) \\ &= (-252.69) - (-242.77) - (-9.85) = -0.11 \text{ eV} \end{aligned} \tag{12}$$

The adsorption energy for O_2 was calculated at -0.11 eV. This shows a weak adsorption of O_2 to the surface. Although modelling was carried out in the gas phase, experimentally an acidic electrolyte was used, so is in actual fact a liquid phase reaction. Bearing this in mind it is assumed the aqueous electrolyte will have a stabilisation effect of around -0.30 eV associated with it [31, 32]. If the reaction had therefore been modelled as liquid phase then the adsorption energy would be around -0.40 eV therefore significantly increasing its stability. To further explain this stabilization effect, imagine that the H_2O/electrolyte solution is acting as a cage of hydrogen bonding over the surface. If the O_2 is continually desorbing, this will disrupt the hydrogen bonding network associated with the liquid phase and so O_2 will be more likely to stay adsorbed to the surface with less O_2 rupturing through this network.

11

3.3.2. Step 4- The association of surface O_2 and $O^{\bullet}$ to form O_3

Step 4 of the reaction is the interaction of surface O_2 and surface O. This step is the most challenging of the 4 steps. The formation of O_2 is thermodynamically favoured over O_3 formation. Experimentally, a high potential is required to drive the reaction towards the formation of O_3. Initial calculations proved unsuccessful. Although O_3 was formed the activation barrier was found to be 1.56 eV. MD (molecular dynamic) calculations in the presence of H_2O were carried out to try to further assess the activation barrier. These calculations are time consuming and a minimum of 10,000 iterations are needed to reach converge. Calculations in this case yielded little success and thus were not investigated further.

Rather than forming O_3 via an OH intermediate, the OH was deprotonated prior to the interaction with surface O_2 forming O_3. Step 4, unlike step 3 was carried out in the presence of four H_2O molecules positioned above the β-PbO_2 surface. Instead of running more MD calculations, the basic principles were adopted and geometry optimization calculations determined instead.

1st step: The adsorption of H_2O

Further surface O, which could be achieved by adsorption of H_2O onto the surface at either the free top or bridging site (see below), is still required for step 4 (Reaction 13).

$$O_2 + O^{\bullet} \longrightarrow O_3 \tag{13}$$

The adsorption energy of H_2O can be calculated using equation 14:

$$
\begin{aligned}
\mathbf{E_{ads}(H_2O)} &= E(\text{surface-}H_2O) - E(\text{clean surface}) - E(H_2O) \\
&= (-326.49) - (-311.69) - (-14.22) = -0.59 \text{ eV}
\end{aligned} \tag{14}
$$

The bridging water was found to be more stable than its top-site counterpart. The adsorption energy was calculated at -0.59 eV, suggesting that adsorption was viable and could continue to the deprotonation step.

12

2nd step- The deprotonation to OH and subsequently to O

Upon adsorption of H_2O, a subsequent deprotonation to OH, followed by a second deprotonation to O takes place. The Gibbs free energy change of reaction (ΔG_{rxn}) for each of the deprotonations was calculated using equation 15:

$$\Delta G^0_{rxn} = G(OH) + G(H^+ + e^-) - G(H_2O)$$
$$= (-321.29) + (-3.44) - (-325.90) = 1.17\ eV \tag{15}$$

The ΔG^0_{rxn} requires free energy which can be obtained by calculating the frequency. The ΔG^0_{rxn} for this deprotonation is calculated at 1.17 eV. This value can be used to determine the minimum potential of 1.17 V required for this deprotonation to occur [33], which is in agreement with an experimental onset potential of 1.80 V or above [9].

A second deprotonation will simultaneously occur after the first and so the minimum potential is again calculated using equation 15:

$$= (-316.20) + (-3.44) - (-321.29) = 1.65\ eV$$

The ΔG^0_{rxn} for this deprotonation is calculated at 1.65 eV. Again this value corresponds to the minimum potential of 1.65 V required for deprotonation to surface O.As aforementioned this is below the experimental onset 1.80 V and so will readily take place.

3rd step- The reaction of O_2 and O to form surface O_3

At this point there are both surface O_2 and O present. Like step 3, there will be an IS, TS and FS associated with the step. The IS was surface O_2 and O, the TS shows O_2 and O in close proximity to one another without any bonding and the FS corresponds to surface adsorbed O_3.

Initial state of reaction

In this step the bond distance between O_2 and O was 3.34 Å. Upon completion stable geometric configuration was determined with a total energy of -316.22 eV.

Transition state

13

In this step the bond distance shortened from 3.34 Å in the IS to 1.77 Å in the TS. The energy associated with the TS is -315.81 eV. A frequency calculation was performed to determine if there is an imaginary frequency (f/i). There is one f/i, suggesting the TS is suitable.

The energy barrier (E_{act}) from IS to TS was determined by Equation 16:

$$\mathbf{E_{act}} = E_{TS} - E_{IS}$$
$$\mathbf{E_{act}} = (-315.81) - (-316.22) = 0.41 \text{ eV} \tag{16}$$

The barrier of 0.41 eV can be bypassed with relative ease. Considering the value for O_2 adsorption calculated earlier (equation 12), one would assume that this large difference in energy would prevent the reaction with surface O shown in step 4. When you take into account the water stabilization effect discussed previously, the adsorption of O_2 becomes more substantial (~0.40 eV), thus increasing the time for surface O_2 to react with surface O before desorption. The CE for this system is low, thus only a small portion of O_2 will stay adsorbed long enough to react and form O_3.

In a comparison of O_3H vs O_3, the O_3 pathway is heavily favoured. At 1.56 eV, the O_3H barrier is 1.15 eV higher than for O, which in itself is a massive reduction. This shows the importance of choosing a suitable intermediate; and by deprotonating first before forming O_3 is much more favourable. The major difference is that the reaction of O_2 + O was carried out in the presence of $4H_2O$, whereas the O_3H pathway was not. To make this a viable study, the O_3H pathway was run in the presence of $4H_2O$ and the barrier was lowered to 1.17 eV. This was still much too high and so for this particular catalyst, the O_2 + O pathway (having a barrier of 0.41 eV) will always be favoured.

Final state of reaction

The final state is the formation of O_3 from O_2 and O. The enthalpy change from IS to FS was calculated using equation 17:

$$\Delta \mathbf{H} = E_{FS} - E_{IS}$$
$$= (-316.29) - (-316.22) = -0.07 \text{ eV} \tag{17}$$

14

The enthalpy change from IS to FS is -0.07 eV, suggesting the FS is therefore slightly more stable than the IS in this exothermic reaction (Figure 5).
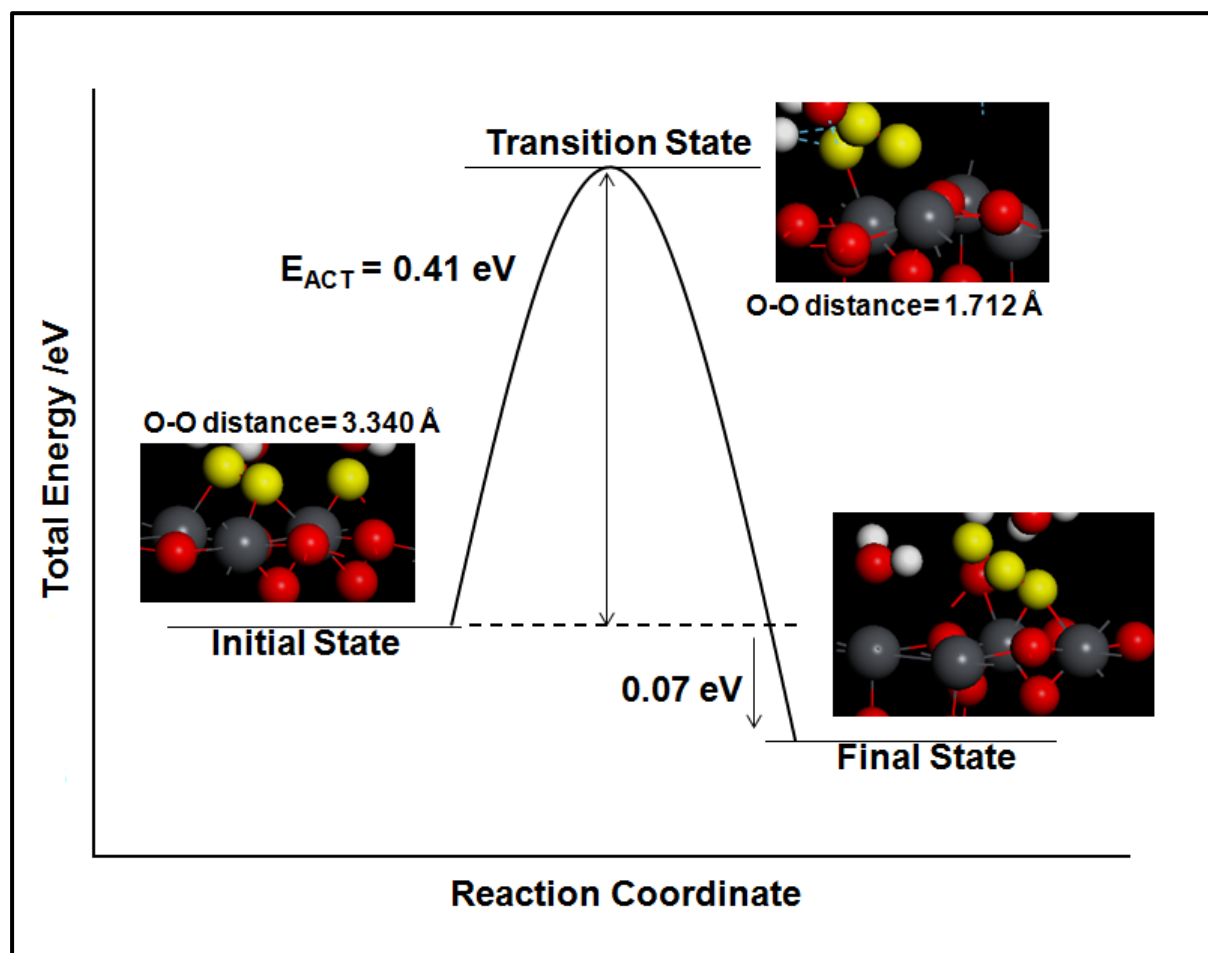

Figure 5. *Energy profile for step 4 of the mechanism: the transformation from O_2 and O to O_3. The atoms highlighted in yellow are the interacting O atoms in the mechanism. The first shows surface O_2 and O, the second shows the O_2 desorbed with O still adsorbed, and the third shows O_3 adsorbed on the surface*

4. Conclusions

This work represents a first theoretical attempt at gaining an insight into O_3 production from water splitting via electrochemistry. Using Density Functional Theory calculations we were able to model possible ozone formation pathways and verify a favourable mechanism. By taking a β-PbO_2 (110) surface as a model catalyst, we have identified a feasible path where H_2O adsorbed onto the surface and was oxidized to form surface OH then O, the latter

15

reacted with a surface bridging O to form O_2 which in turn reacted with further surface O to form O_3.

References

[1] U.E.P. Agency, Office of Water, (1999) 4607.

[2] C. Zwiener, F.H. Frimmel, Oxidative treatment of pharmaceuticals in water, Water Research, 34 (2000) 1881-1885.

[3] R.J. Bull, L.S. Birnbaum, K.P. Cantor, J.B. Rose, B.E. Butterworth, R. Pegram, J. Tuomisto, Water Chlorination: Essential Process or Cancer Hazard?, Fundamental and Applied Toxicology, 28 (1995) 155-166.

[4] F. L, The Application of Ozone Technology for Public Health and Industry, White Paper, (2005).

[5] M.X. Meng, J.S. Hsieh, J. Tappi, 83 (2000) 6772.

[6] D. Iliadis, B.J. Millar, Ozone and its use in periodontal treatment, Open Journal of Stomatology, 3 (2013) 197-202.

[7] J. Lee, B. Jeong, J.D. Ocon, Oxygen electrocatalysis in chemical energy conversion and storage technologies, Current Applied Physics, 13 (2013) 309-321.

[8] J. Wang, Electrochemical Glucose Biosensors, Chemical Reviews, 108 (2008) 814-825.

[9] P.A. Christensen, W.F. Lin, H. Christensen, A. Imkum, J.M. Jin, G. Li, C.M. Dyson, Room Temperature, Electrochemical Generation of Ozone with 50% Current Efficiency in 0.5M Sulfuric Acid at Cell Voltages < 3V, Ozone: Science & Engineering, 31 (2009) 287-293.

[10] P.C. Foller, C.W. Tobias, The Anodic Evolution of Ozone, Journal of The Electrochemical Society, 129 (1982) 506-515.

[11] L.M. Da Silva, L.A. De Faria, J.F.C. Boodts, Electrochemical ozone production: influence of the supporting electrolyte on kinetics and current efficiency, Electrochimica Acta, 48 (2003) 699-709.

[12] R. Amadelli, L. Armelao, A.B. Velichenko, N.V. Nikolenko, D.V. Girenko, S.V. Kovalyov, F.I. Danilov, Oxygen and ozone evolution at fluoride modified lead dioxide electrodes, Electrochimica Acta, 45 (1999) 713-720.

[13] I. Awad M, M. Saleh M, T. Ohsaka, Journal of Electrochemical Society, 153 (2006) D207-D212.

[14] L.M. Da Silva, D.V. Franco, L.A. De Faria, J.F.C. Boodts, Surface, kinetics and electrocatalytic properties of $Ti/(IrO_2 + Ta_2O_5)$ electrodes, prepared using controlled cooling rate, for ozone production, Electrochimica Acta, 49 (2004) 3977-3988.

[15] A. Kraft, M. Stadelmann, M. Wünsche, M. Blaschke, Electrochemical ozone production using diamond anodes and a solid polymer electrolyte, Electrochemistry Communications, 8 (2006) 883-886.

[16] K. Arihara, C. Terashima, A. Fujishima, Electrochemical and Solid-State Letters, 9 (2006) D17-D20.

[17] Y. Wang, H., S. Cheng, K.-Y. Chan, X.Y. Li, Electrolytic Generation of Ozone on Antimony- and Nickel-

Doped Tin Oxide Electrode, Journal of Electrochemical Society, 152 (2005) D197-D200.

[18] H. Shekarchizade, M.K. Amini, International Journal of Electrochemistry, (2011) 1-13.

[19] S. Cheng, K.-Y. Chan, Electrochemical and Solid-State Letters, 7 (2007) D4-D6.

[20] G. Kresse, J. Hafner, Ab initio molecular dynamics for liquid metals, Physical Review B, 47 (1993) 558-561.

[21] G. Kresse, J. Hafner, Ab initio molecular dynamics for open-shell transition metals, Physical Review B, 48 (1993) 13115-13118.

[22] G. Kresse, J. Hafner, Ab initio molecular-dynamics simulation of the liquid-metal–amorphous-semiconductor transition in germanium, Physical Review B, 49 (1994) 14251-14269.

[23] P.E. Blöchl, Projector augmented-wave method, Physical Review B, 50 (1994) 17953-17979.

[24] J.P. Perdew, K. Burke, M. Ernzerhof, Generalized Gradient Approximation Made Simple, Physical Review Letters, 77 (1996) 3865-3868.

[25] M. Methfessel, A.T. Paxton, High-precision sampling for Brillouin-zone integration in metals, Physical Review B, 40 (1989) 3616-3621.

[26] H.J. Monkhorst, J.D. Pack, Special points for Brillouin-zone integrations, Physical Review B, 13 (1976) 5188-5192.

[27] A. Alavia, P. Hu, T. Deutsch, P.L. Sylvestrelli, J. Hutter, Journal of Physical Review Letters, 80 (1998) 3650-3653.

[28] A. Michaelides, P. Hu, Insight into Microscopic Reaction Pathways in Heterogeneous Catalysis, Journal of the American Chemical Society, 122 (2000) 9866-9867.

[29] Z.-P. Liu, P. Hu, General Rules for Predicting Where a Catalytic Reaction Should Occur on Metal Surfaces: A Density Functional Theory Study of C−H and C−O Bond Breaking/Making on Flat, Stepped, and Kinked Metal Surfaces, Journal of the American Chemical Society, 125 (2003) 1958-1967.

[30] I. Petersson, E. Ahlberg, B. Berghult, Parameters influencing the ratio between electrochemically formed α- and β-PbO_2, Journal of Power Sources, 76 (1998) 98-105.

[31] R. Kavanagh, X.-M. Cao, W.-F. Lin, C. Hardacre, P. Hu, Origin of Low CO_2 Selectivity on Platinum in the Direct Ethanol Fuel Cell, Angewandte Chemie International Edition, 51 (2012) 1572-1575.

[32] T. Song, P. Hu, Insight into the solvent effect: A density functional theory study of cisplatin hydrolysis, The Journal of Chemical Physics, 125 (2006) 091101.

[33] W.-F. Lin, S.-G. Sun, Z.-Q. Tian, Z.-W. Tian, Quantum chemistry and in situ FTir spectroscopy studies on potential-dependent properties of CO adsorbed on Pt electrodes, Electrochimica Acta, 38 (1993) 1107-1114.

Graphical Abstract

$$3H_2O \rightarrow O_3 + 6H^+ + 6e^-$$
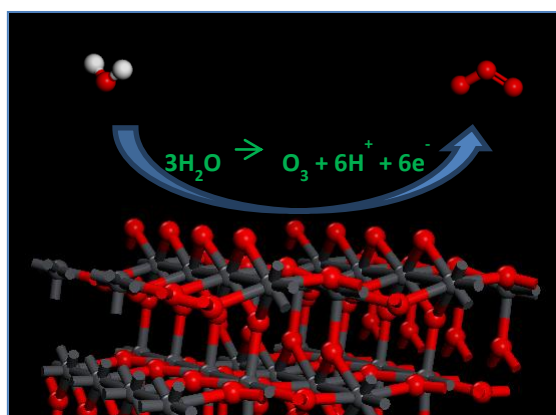
Highlights

- Mechanisms for ozone production via splitting of water identified by DFT modelling

- H_2O adsorbed onto the electrode was oxidized to form surface OH then O

- Eley-Rideal style interaction between O_2 and surface O to form O_3

- A different reaction pathway via an O_3H intermediate was less favoured

Highlights